CONFIDENTIAL

Copy
RM E58E16

NACA RM E58E16

NACA

# RESEARCH MEMORANDUM



## PERFORMANCE OF AN ISENTROPIC, ALL-INTERNAL-CONTRACTION, AXISYMMETRIC INLET DESIGNED FOR MACH 2.50

By David N. Bowditch and Bernhard H. Anderson

Lewis Flight Propulsion Laboratory
Cleveland, Ohio

[redacted]



NATIONAL ADVISORY COMMITTEE
FOR AERONAUTICS

WASHINGTON

September 15, 1958

CONFIDENTIAL

NATIONAL ADVISORY COMMITTEE FOR AERONAUTICS

RESEARCH MEMORANDUM

# PERFORMANCE OF AN ISENTROPIC, ALL-INTERNAL-CONTRACTION, AXISYMMETRIC INLET DESIGNED FOR MACH 2.50*

By David N. Bowditch and Bernhard H. Anderson

## SUMMARY

An experimental investigation of an internal-contraction, axially symmetric inlet with isentropic compression surfaces on both the cowl and centerbody was conducted over a range of Mach numbers from 2.0 to 2.7 at angles of attack from $0^{\circ}$ to $6^{\circ}$. The study was made to determine the optimum bleed system, together with a method of controlling the inlet.

At Mach 2.5, bleeding of about 0.3 percent by means of perforations ahead of the throat allowed a 3-percent-larger running contraction ratio than could be obtained with no supersonic bleed and permitted the centerbody to retract to the design position. The best subsonic bleed system consisted of flush slots located opposite each other on the cowl and centerbody just downstream of the throat. By bleeding 13 percent with this system, a peak recovery of 0.91 was obtained at Mach 2.5. Cowl static pressures ahead of these slots appeared to be satisfactory for sensing the normal-shock position. However, the centerbody position would have to be scheduled with Mach number, angle of attack, and Reynolds number since no pressure signal was found that would permit prediction of critical internal contraction.

## INTRODUCTION

External-compression inlets are capable of efficient compression at Mach numbers above 2.0, but the wave drag associated with the external cowl tends to be high. One approach to eliminate high cowl wave drag is to use all-internal-compression-type inlets with low cowl angles, such as in references 1 and 2.

The problems associated with the operation of internal-compression inlets are numerous. To investigate some of these problems, the test at Ames laboratory of an internal-compression axisymmetric inlet was extended in the Lewis 10- by 10-foot wind tunnel (refs. 3 and 4). Of primary

---

* Title, Unclassified

interest in this investigation was the effect of various bleed configurations on the operating characteristics of the inlet, the effect of off-design operation, and the evaluation of a control parameter for optimizing inlet performance.

## SYMBOLS

| | |
|---|---|
| $A$ | flow area |
| $A_l$ | annular cowl-lip flow area |
| $A_{in}$ | inlet capture area |
| $A_{th}$ | throat area |
| $M$ | Mach number |
| $P$ | total pressure |
| $\overline{P}$ | average total pressure |
| $\Delta P$ | difference between maximum and minimum total pressures at a station |
| $p$ | static pressure |
| $R$ | cowl radius at station 2 |
| $r$ | radial distance from inlet centerline |
| $Re$ | Reynolds number |
| $\alpha$ | angle of attack |

Subscripts:

| | |
|---|---|
| 0 | free stream |
| 1 | cowl lip |
| 2 | inlet throat station at design centerbody position |
| 3 | diffuser inlet |
| 4 | flow measuring station 14 in. upstream of choked area |

## APPARATUS AND PROCEDURE

The inlet was investigated in the 10- by 10-foot supersonic wind tunnel at Mach numbers of 1.99, 2.10, 2.20, 2.30, 2.40, 2.50, 2.59, and 2.69 and Reynolds numbers per foot of $2.5\times10^6$, $1.5\times10^6$, and $0.64\times10^6$. Angle of attack was varied from $0^\circ$ to $6^\circ$.

The theoretical contour of the supersonic compression surfaces of the inlet was determined by using axially symmetric characteristics. The flow was assumed to be Mach 2.5 in the free stream and 1.20 at the throat. Previous experimental tests of a similar inlet had indicated that a throat Mach number as low as 1.2 could not be obtained and that considerable boundary-layer buildup occurred on the compression surfaces. The throat area was increased to 113.2 percent of the theoretical area to allow for these conditions. The area increase was diminished with distance upstream of the throat and became zero at the spike tip and cowl lip.

Two inlets differing only in supersonic diffuser length were designed by this method and will hereafter be called the original long inlet and the short inlet. The longer inlet had about one third the maximum pressure gradient and twice the length from cowl lip to throat of the short inlet. After testing the original long inlet, enlargement of the throat area an additional 2 percent by reducing the centerbody diameter was found to be desirable. The long inlet with the 2-percent-larger throat area shall hereafter be called the modified long inlet.

A cutaway view of the inlet showing the supersonic compression surfaces and the optimum subsonic bleed located in the intermediate section is presented in figure 1. The several bleed configurations tested included perforated bleed in the supersonic and subsonic parts of the diffuser, and flush slots at two locations in the subsonic diffuser. The configurations for which data are presented are shown in figure 2. Figure 2(a) shows the basic inlet with no bleed, while figure 2(b) shows the long and short inlets with the constant-Mach-number section and supersonic perforated bleed. The subsonic slots and perforations were always tested in combination with approximately 1 percent bleed through supersonic cowl perforations to the free stream, as shown in figures 2(c) and (d). Also shown in figure 2 are the locations of stations 1, 2, and 3 corresponding to the cowl lip, throat, and diffuser exit. Station 4, the mass-flow measuring station, is located 14 inches ahead of the choked exit.

The rear part of the model contained plugs for controlling the main flow as well as spike- and cowl-bleed flows. The intermediate part of the model in the region of the throat could be assembled so that either bleed slots, perforated bleed, a constant-Mach-number section, or some

combinations of these could be included. The forward cowl-bleed slot, with the supersonic part of the cowl and spike removed, is shown in figure 3(a), and the three centerbody constant-Mach-number sections containing the forward and rear slots and perforated bleed are shown in figure 3(b). The inlet supersonic compression surfaces of the cowl and centerbody attach to the front of the intermediate section, as shown in figure 1. Both the centerbody tip and the cowl lip were roughened by grooves to try to induce early transition.

The bleed-slot dimensions are given in figure 4. The areas of perforated bleed consist of 1/8-inch-diameter holes drilled perpendicular to the inlet centerline. The holes were staggered from row to row (as seen in fig. 3(b)) with 0.188 inch between hole centers in each row. The distance between centerlines of two adjacent circumferential rows was 3/16 inch. Perforated bleed could be located anywhere in the region from 1.4 inches ahead of the throat to 8.0 inches downstream of the throat on the cowl and 10 inches downstream of the throat on the centerbody.

The internal-flow area for various centerbody positions is given in figure 5 for the configurations of primary interest. The coordinates for the short inlet and the two long inlets are presented in table I. These coordinates include the constant-Mach-number section between 1.2 and 5.2 inches behind the throat. When the constant-Mach-number section was not in use, the small step on the centerbody indicated by the coordinates in table I was faired.

The inlet pressure recovery and distortions were measured at the diffuser exit (station 3) with 36 area-weighted total-pressure tubes (in six rakes) and six wall static-pressure orifices. Distortions were calculated by taking the difference between the maximum and minimum total pressures and dividing by the average. Static orifices were located on the inner cowl surface from 1.5 inches downstream of the cowl lip to downstream of the throat. The centerbody had no pressure instrumentation because of the difficulties imposed by the large translation of the entire centerbody. The conditions at station 2 were measured by eight total-pressure tubes in a rake and three static-pressure orifices. Throat Mach numbers were calculated from the ratio of the average total pressure from the rake to the average static pressure. The rakes at stations 2 and 3 and the cowl orifices can be seen in figure 1.

Main-duct and bleed-duct mass flows were calculated by using six static orifices located at station 4 and by assuming isentropic one-dimensional flow between stations 4 and the known choked-discharge area. The bleed-flow recoveries were measured by two 19-tube area-weighted rakes, located at station 4, in both the centerbody- and cowl-bleed ducts.

Static-pressure variations were obtained from three pressure transducers located ahead of the forward cowl-bleed slot and one located just behind the cowl slot. Signals from these transducers and the exit-plug position were recorded on an optical oscillograph, while the plug was opened from the peak-recovery position and then closed until the inlet went subcritical. Plug position and inlet recovery were correlated so that a plot of pressure signal against recovery could be obtained.

## RESULTS AND DISCUSSION

### General Inlet Performance

The performance of the short inlet was poor because its centerbody could not be retracted into the design position without subcritical operation up to a free-stream Mach number of 2.7. With the inlet started, maximum obtainable contraction remained approximately constant from Mach 2.4 to 2.7, even though the corresponding allowable isentropic contraction increased about 30 percent. Throat-rake measurements showed a large low-energy-air region on the spike, which indicates that some kind of shock boundary-layer interaction was always encountered at this minimum spike extension. The short inlet was not investigated further because of this starting problem.

The peak-pressure-recovery performance of the long inlet is presented in figure 6. At Mach 2.5 with no bleed (open circles) the centerbody of the original inlet could be retracted to only 0.42 inlet diameter ahead of the design position while the inlet remained started. The addition of a small amount of perforated bleed upstream of the throat (solid circles) allowed the spike to be fully retracted with the resulting increase in pressure recovery from 0.79 to 0.845. The best subsonic bleed configuration (squares) further increased the recovery to 0.91 and decreased the distortion from 0.31 to 0.12. This configuration obtained similar gains at Mach 2.6, but at Mach 2.0 it gave a lower total-pressure recovery than the configuration with no constant-Mach-number section in spite of the fact that it had no bleed. The better performance is believed due to the better alinement of the compression surfaces at the maximum contracted condition when no constant-Mach-number section was included. Another factor is that the bleeds were not located in the most effective area, the throat, when the centerbody was extended about 1.2 inlet diameters for Mach 2 operation.

With no subsonic bleed, the use of the constant-Mach-number section gave conflicting results. For example, the maximum obtainable recovery at design centerbody position was increased 1.5 percent by using the section at Mach 2.6, while it dropped 1 percent at Mach 2.5 (fig. 6). At Mach 2.5, a configuration with no constant-Mach-number section but

with two rows of perforations on the centerbody opposite the forward cowl slot was run to determine the effect of the constant-Mach-number section with good subsonic bleed, and no measurable effect was observed. Based on these observations, the constant-Mach-number section does not seem to appreciably increase the recovery at Mach 2.5, and the additional extension required by the section decreased the recovery at Mach 2.0.

Increasing the throat area 2 percent over that of the original inlet did not change the maximum obtainable contraction ratio ($A_c/A_T$) of about 2.2 with the inlet started at Mach 2.5. A contraction ratio of 2.22 was needed to retract the spike of the modified inlet to the design position, however, so that neither inlet could operate under started conditions with the centerbody fully retracted. When both long inlets were run in the design position with the addition of perforated bleed ahead of the throat, they both obtained the same throat recoveries at peak-inlet-recovery conditions. The Mach number calculated at the throat at these conditions was less for the modified inlet, even though its throat area was 2 percent larger. With the normal shock well downstream, however, the throat Mach number of the modified inlet increased until it was higher than that of the original inlet, which was little affected by shock position. It therefore appears that the terminal shock affected the flow ahead of the throat of the modified inlet in such a manner that both inlets obtained essentially the same throat recovery. All further data are for the modified long inlet unless otherwise indicated.

The inlet was sensitive to centerbody position as shown in figure 6, where at Mach 2.5 an extension of 0.42 inlet diameter caused a loss of 2.0 to 3.5 counts in total-pressure recovery. The corresponding change in contraction ratio ($A_{in}/A_{th}$) from 2.22 to 2.18 changes the calculated recovery only 1 percent. Figure 7(a) presents a comparison between the theoretical (isentropic) pressure distribution and the experimental pressure distributions for the two points A and B in figure 6. The design condition (point A) shows a smooth inlet pressure distribution and good agreement with the theoretical prediction. Off-design centerbody position (point B), however, causes large variations in pressure from the theoretical curve, as shown in figure 7(a). This poor pressure distribution increased the cowl boundary-layer thickness at station 2, as illustrated by the total-pressure profile in figure 7(b).

The effect of angle of attack on peak pressure recovery is presented in figure 8. At zero angle of attack and a free-stream Mach number of 2.5, a pressure recovery of 91 percent was obtained. Increasing the angle of attack to $3^\circ$ caused the recovery to drop to 88.8 percent. The spike position for both these conditions was the design position for Mach 2.5.

A similar trend existed at Mach 2.0, where peak pressure recovery decreased from 86 percent at zero angle of attack to 78.3 percent at 6° angle of attack.

During the test, it was observed that the inlet remained supercritical at the design contraction ratio ($A_{in}/A_{th}$ = 2.22) up to an angle of attack of 4.75° at Mach 2.5, after which the inlet became subcritical. The maximum contraction ratio that could be obtained at 6° angle of attack was 2.175, which corresponds to a centerbody extension of 0.575 inlet diameter ahead of the design position. At Mach 2.0, an extension of 0.061 inlet diameter from the minimum obtainable at $\alpha = 0°$ was required to reach $\alpha = 6°$, as seen in figure 8.

The effect of Reynolds number on the maximum obtainable contraction ratio is shown in figure 9. A decrease in Reynolds number from $2.5\times10^6$ to $0.64\times10^6$ per foot required a centerbody extension of 0.60 inlet diameter in order to maintain supercritical flow. This is a large centerbody translation, but it represents a change of only 3 percent in the contraction ratio. The Reynolds number change is much larger than would be encountered on an actual aircraft during maximum flight speed, but it illustrates that it may be necessary to account for this effect.

When the normal shock is regurgitated, a large spike translation and an increase in airflow is required to start the inlet. The starting contraction ratios ($A_l/A_{th}$) for one of the configurations tested are shown in figure 10. The maximum theoretical contraction ratio based on free-stream Mach number is shown for comparison. The ability of the inlet to start with more contraction than that predicted by the free-stream Mach number is probably due to the separation on the centerbody, as shown in figure 11(g). This separation spilled flow around the inlet cowl lip while the inlet was unstarted, but disappeared just as the inlet started.

Schlieren pictures of the inlet during the starting cycle at Mach 2.50 are given in figure 11. Figure 11(a) shows the inlet just after the shock was lost and before the back pressure was reduced. Under these conditions the inlet obtains normal-shock recovery of about 0.50 and is unstable. The instability, measured with the spike in the design position just after the shock was lost, was found to be random. Two separate measurements at the cowl-bleed slot indicated amplitudes of 3 and 6 percent of the free-stream total pressure. The flow was intermittently stable, as in figures 11(c), (f), and (g), and unstable as shown by the waviness of the shock waves in figures 11(a), (b), (d), and (e) when the centerbody was extended. The inlet went supercritical at a centerbody extension of 1.337 inlet diameters, which was indicated by the disappearance of the separated flow region on the centerbody between figures 11(g) and (h). The inlet in the running condition at Mach 2.5 is shown in figure 11(i).

## Bleed Performance

Supersonic perforated bleed upstream of the throat of only about 0.3 percent of the capture mass flow was required to retract the spike of the original long inlet into the design position at Mach 2.5. The bleed thus allowed an increase in the contraction ratio of 3 percent and therefore accomplished what a 2-percent increase in throat area could not. Figure 12, which presents the performance of the bleed systems tested, shows that an increase above this minimum amount of supersonic bleed had little effect on the inlet pressure recovery. Static pressures in the throat region indicated that additional supersonic bleed also badly distorted the flow. All subsonic slot and perforated bleed configurations that could be retracted into the design position bled approximately 1 percent ahead of the throat to the free stream.

In addition to the supersonic bleed performance, figure 12 also presents the peak inlet recovery, bleed-flow recovery, and inlet distortion as a function of cowl- and spike-bleed flow for the subsonic bleed configurations. The most successful bleed system, consisting of the original forward slots, obtained the highest inlet recovery with a relatively low bleed flow. The inlet recovery increased linearly with cowl-bleed flow from $\overline{P}_3/P_0 = 0.847$ until the cowl bleed choked at $\overline{P}_3/P_0 = 0.91$, as can be seen by the bleed recovery decreasing sharply at 0.09 bleed flow. The distortion decreased from 0.23 to 0.115, while the bleed flow was increased over the same range. Enlarging the cowl bleed did not affect the bleed performance below a bleed-mass-flow ratio of 0.07, but above this the performance dropped below that of the original forward slot and never quite reached an inlet recovery of 0.91 in spite of bleed-mass-flow ratios up to 0.126. However, the bleed recovery was greatly increased and the inlet distortion was slightly improved by enlarging the cowl-bleed slot. Moving the slots back to the rear position increased the bleed flow required for a given pressure recovery. The cowl-bleed recovery improved over that for the original forward slot, but not as much as with the enlarged forward slot. Also, the distortion was considerably higher for the rear slots than for either of the forward slots. The forward and rear centerbody slots both produced about the same performance except that the slot in the rear position did not choke at as low a weight flow.

The subsonic perforated bleed produced about the same inlet recovery as the forward slots up to a bleed mass flow of about 0.04 and a recovery of 0.875. Additional bleed flow improved the distortion but had little effect on the inlet recovery. The bleed-flow recoveries were poor for this bleed system.

The static pressure at Mach 2.5 in the vicinity of the forward slots is shown in figure 13, where it is plotted as a function of inlet recovery.

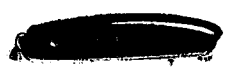

Probe D indicates that the shock train begins to reach the forward slot at an inlet pressure recovery of 0.83, which is the peak recovery with no subsonic bleed. The shock train consolidates on the bleed, as indicated by a continued increase in probe D pressure; and its effects are not felt forward of the slot until a recovery of 0.886 is reached, as shown by probes A, B, and C. At inlet pressure recoveries above 0.886, the static pressure ahead of the slot increased until the inlet became subcritical at a recovery of about 0.91. The noise indicated in the figure is the amplitude of a high-frequency oscillation observed when the static probes began to indicate the effects of the shock.

## Inlet Control

The control of this inlet presents two problems: the control of the normal or terminal shock, and the positioning of the centerbody for optimum internal contraction. The normal-shock position can be controlled by a bypass that will have to be fairly large to meet starting and off-design weight-flow requirements. These requirements are illustrated by the corrected weight flow at station 3 increasing 45 percent during starting at Mach 2.5, and being 31 percent higher at peak-recovery conditions at Mach 2.0 than at the same conditions at Mach 2.5. The static pressure ahead of the forward slot produced a potentially useful bypass-control signal, as seen from figure 13. No control-signal data were taken at off-design spike positions and Mach numbers.

In the previous discussion of angle-of-attack performance, it was shown that to reach $\alpha = 6^{\circ}$ with the inlet supercritical, the centerbody would have to be extended ahead of the peak-recovery position at zero degrees. This centerbody extension would cause a loss in recovery at $\alpha = 0^{\circ}$ of 2 and 4 counts at Mach 2.0 and 2.5, respectively. The centerbody of this inlet therefore must be positioned as a function of angle of attack to obtain good performance. Also, to obtain good inlet performance, the control will have to account for Reynolds number, as can be seen from the data presented in figure 9.

The centerbody translation required by the change in Mach number from 2.5 to 2.0 is 1.32 inlet diameters for the long inlet with constant-Mach-number section, as illustrated in figure 6. To have essentially no internal contraction for transonic operation, this configuration would require an extension of about 2 inlet diameters. This extension could be reduced to 1.14 and 1.56 for Mach 2.0 and approximately no contraction conditions, respectively, by removing the constant-Mach-number section. This centerbody movement would probably have to be scheduled with Mach number, as no internal pressure signals were observed that would predict the optimum internal contraction.

## SUMMARY OF RESULTS

An all-internal-contraction isentropic inlet was tested in the 10- by 10-foot wind tunnel with the following results:

1. At Mach 2.5, the inlet recovery was increased from 0.83 to 0.91 by bleed of 0.13 of the inlet mass flow by means of flush slots just downstream of the throat.

2. Bleed forward of the throat was very effective in permitting retraction of the spike into the design position. However, increasing the amount of this bleed beyond the minimum required for spike retraction had little effect on the inlet pressure recovery.

3. Centerbody position would have to be scheduled with angle of attack and Reynolds number as well as flight Mach number in order to avoid significant losses in inlet pressure recovery.

4. The static pressures in the throat forward of the flush slots appeared to be potentially useful for controlling the inlet normal-shock position at Mach 2.5 and zero angle of attack.

Lewis Flight Propulsion Laboratory
National Advisory Committee for Aeronautics
Cleveland, Ohio, May 22, 1958

## REFERENCES

1. Mossman, Emmet A., and Pfyl, Frank A.: An Experimental Investigation at Mach Numbers from 2.1 to 3.0 of Circular-Internal-Contraction Inlets with Translating Centerbodies. NACA RM A56G06, 1956.

2. Kepler, C. E.: Performance of a Variable-Geometry Chin Inlet at Mach Numbers from 1.6 to 3.0. Res. Dept., Rep. R-0955-24, United Aircraft Corp., Oct. 1957. (Contract NOa(s)55-133-c.)

3. Hubbartt, J. E.: Preliminary Investigation of Isentropic Internal Contraction Inlets. Rep. LR.12229, Lockheed Aircraft Corp., Sept. 20, 1957.

4. Rozycki, R. C.: Experimental Investigation of Isentropic Internal Contraction Inlets at Mach Numbers from 2.00 to 2.70. Rep. LR 12565, Lockheed Aircraft Corp., Oct. 10, 1957.

TABLE I. - COWL AND CENTERBODY COORDINATES

[Constant-Mach-number section included between 1.20 and 5.20 inches behind throat.]

| Coordinates | | | | | | | | |
|---|---|---|---|---|---|---|---|---|
| Long centerbody | | | Short centerbody | | Long cowl | | Short cowl | |
| Distance ahead of throat, in. | Original spike radius, in. | Modified spike radius, in. | Distance ahead of throat, in. | Spike radius, in. | Distance ahead of throat, in. | Cowl radius, in. | Distance ahead of throat, in. | Cowl radius, in. |
| 18.73 | 0 | 0 | 12.14 | 0 | 14.55 | 4.466 | 7.60 | 4.517 |
| 18.00 | .030 | .023 | 11.75 | .025 | 14.00 | 4.466 | 6.75 | 4.517 |
| 17.00 | .109 | .095 | 10.75 | .122 | 13.00 | 4.463 | 5.75 | 4.504 |
| 16.00 | .203 | .201 | 9.75 | .261 | 12.00 | 4.459 | 4.75 | 4.451 |
| 15.00 | .332 | .328 | 8.75 | .432 | 11.00 | 4.444 | 3.75 | 4.356 |
| 14.00 | .475 | .467 | 7.75 | .630 | 10.00 | 4.413 | 2.75 | 4.219 |
| 13.00 | .625 | .615 | 6.75 | .854 | 9.00 | 4.370 | 2.00 | 4.102 |
| 12.00 | .783 | .771 | 5.75 | 1.102 | 8.00 | 4.319 | 1.75 | 4.068 |
| 11.00 | .949 | .935 | 4.75 | 1.364 | 7.00 | 4.262 | 1.00 | 3.992 |
| 10.00 | 1.123 | 1.106 | 3.75 | 1.645 | 6.00 | 4.201 | .50 | 3.962 |
| 9.00 | 1.305 | 1.286 | 2.75 | 1.954 | 5.00 | 4.139 | 0 | 3.949 |
| 8.00 | 1.494 | 1.475 | 2.00 | 2.199 | 4.00 | 4.079 | | |
| 7.00 | 1.693 | 1.673 | 1.00 | 2.490 | 3.00 | 4.023 | Cylindrical rear of throat | |
| 6.00 | 1.905 | 1.878 | 0 | 2.602 | 2.00 | 3.979 | | |
| 5.00 | 2.101 | 2.073 | | | 1.00 | 3.954 | | |
| 4.00 | 2.275 | 2.246 | Same as long centerbody rear of throat | | 0 | 3.949 | | |
| 3.00 | 2.414 | 2.383 | | | | | | |
| 2.00 | 2.509 | 2.478 | | | Cylindrical rear of throat | | | |
| 1.00 | 2.565 | 2.532 | | | | | | |
| 0 | 2.602 | 2.568 | | | | | | |
| -1.00 | 2.592 | 2.558 | | | | | | |
| -2.00 | 2.582 | 2.548 | | | | | | |
| -3.00 | 2.572 | 2.538 | | | | | | |
| -4.00 | 2.561 | 2.527 | | | | | | |
| -5.00 | 2.547 | 2.513 | | | | | | |
| -6.00 | 2.520 | 2.489 | | | | | | |
| -8.00 | 2.426 | 2.408 | | | | | | |
| -10.00 | 2.297 | 2.287 | | | | | | |
| -11.94 | 2.139 | 2.139 | | | | | | |
| -13.80 | 1.867 | 1.867 | | | | | | |
| -15.80 | 1.710 | 1.710 | | | | | | |
| -16.80 | 1.600 | 1.600 | | | | | | |
| Cylindrical rear of -16.80 | | | | | | | | |

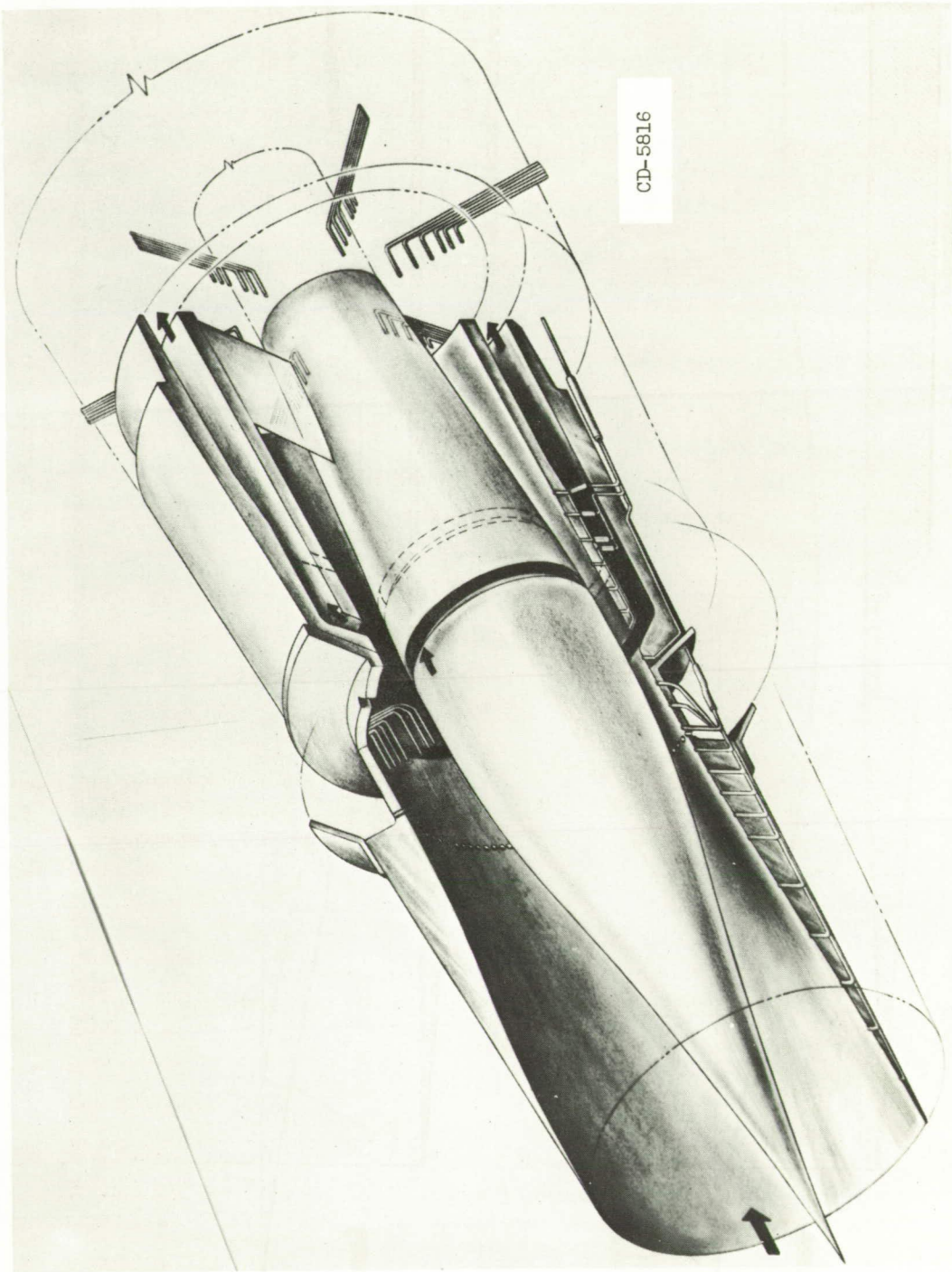


Figure 1. - Long supersonic inlet with intermediate section containing forward flush slots and constant-Mach-number section.

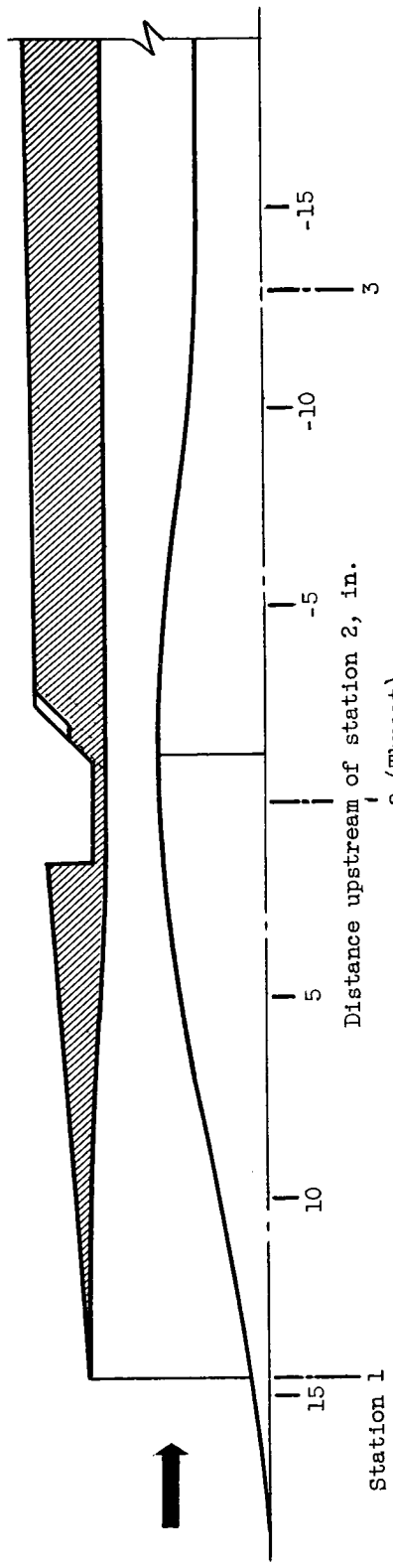


(a) Long inlet.

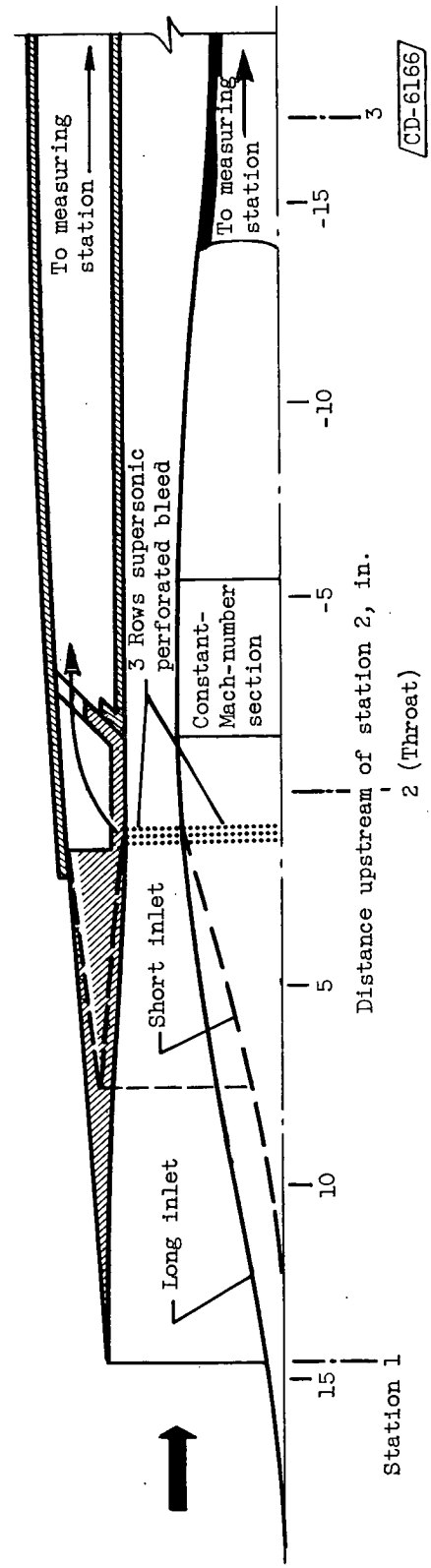


(b) Long and short inlets, constant-Mach-number section, and supersonic perforated bleed.

Figure 2. - Inlet and bleed configurations.

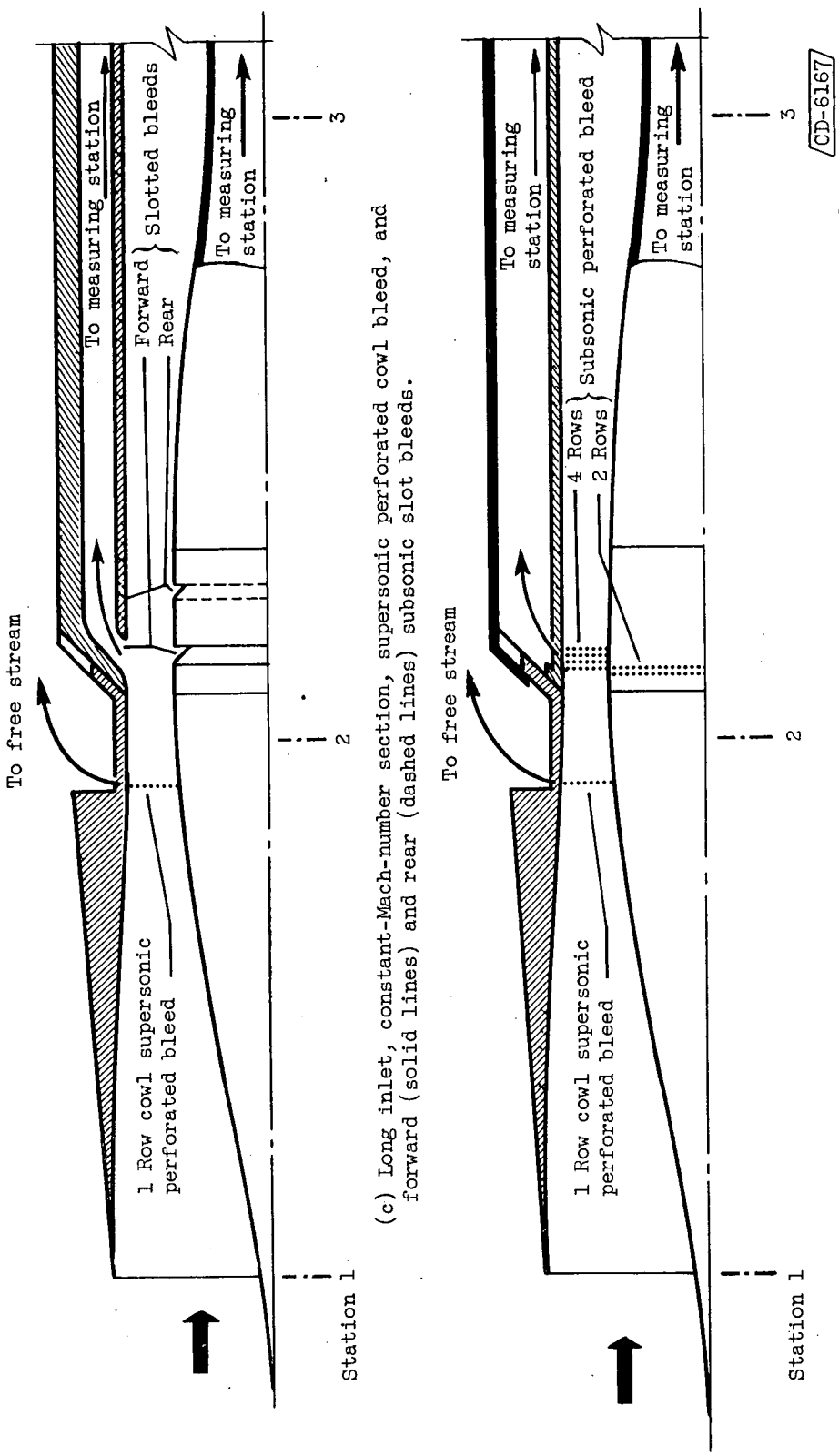


(c) Long inlet, constant-Mach-number section, supersonic perforated cowl bleed, and forward (solid lines) and rear (dashed lines) subsonic slot bleeds.

(d) Long inlet, constant-Mach-number section, supersonic perforated cowl bleed, and subsonic perforated bleed.

Figure 2. - Concluded. Inlet and bleed configurations.

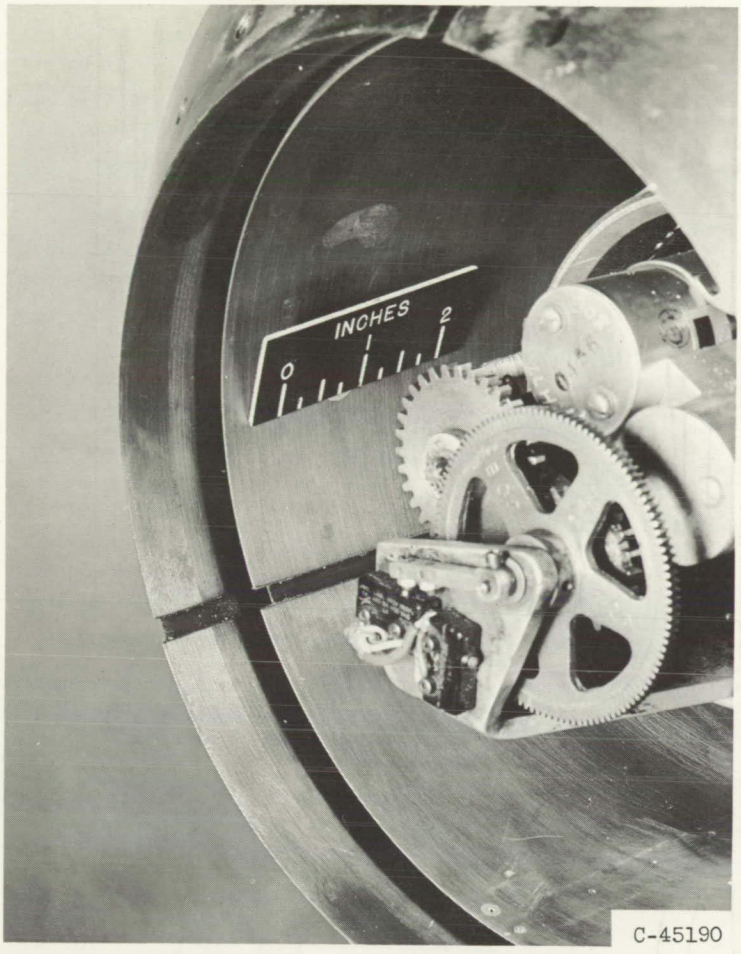


(a) Forward cowl slot with cowl and centerbody removed.


(b) Centerbody constant-area sections showing bleed slots (forward and rear) and perforations.

Figure 3. - Representative parts of bleed configurations.

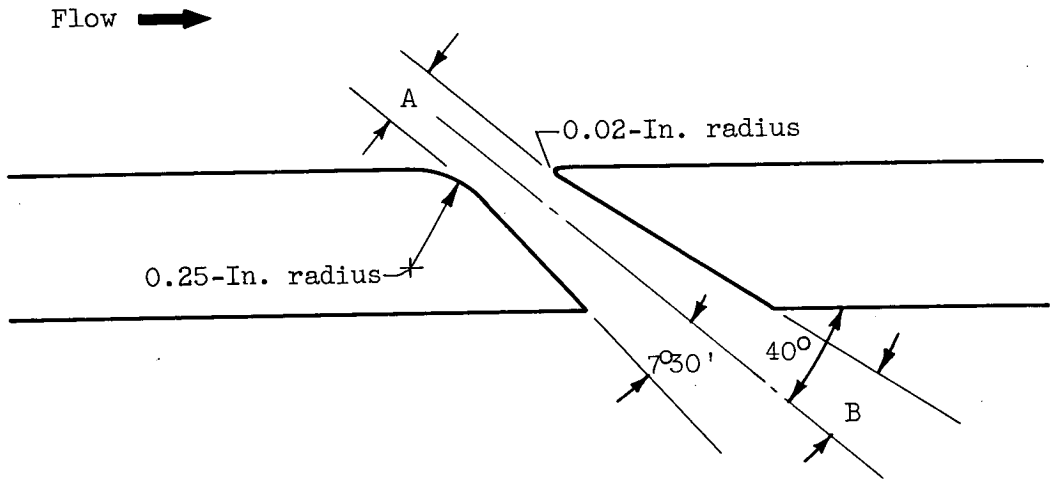


| Bleed slots | A, in. | B, deg |
|---|---|---|
| Centerbody | 0.154 | 7°30' |
| Original cowl (forward and rear) | .154 | 2°30' |
| Enlarged forward cowl | .205 | 2°30' |

Figure 4. - Slot geometry.

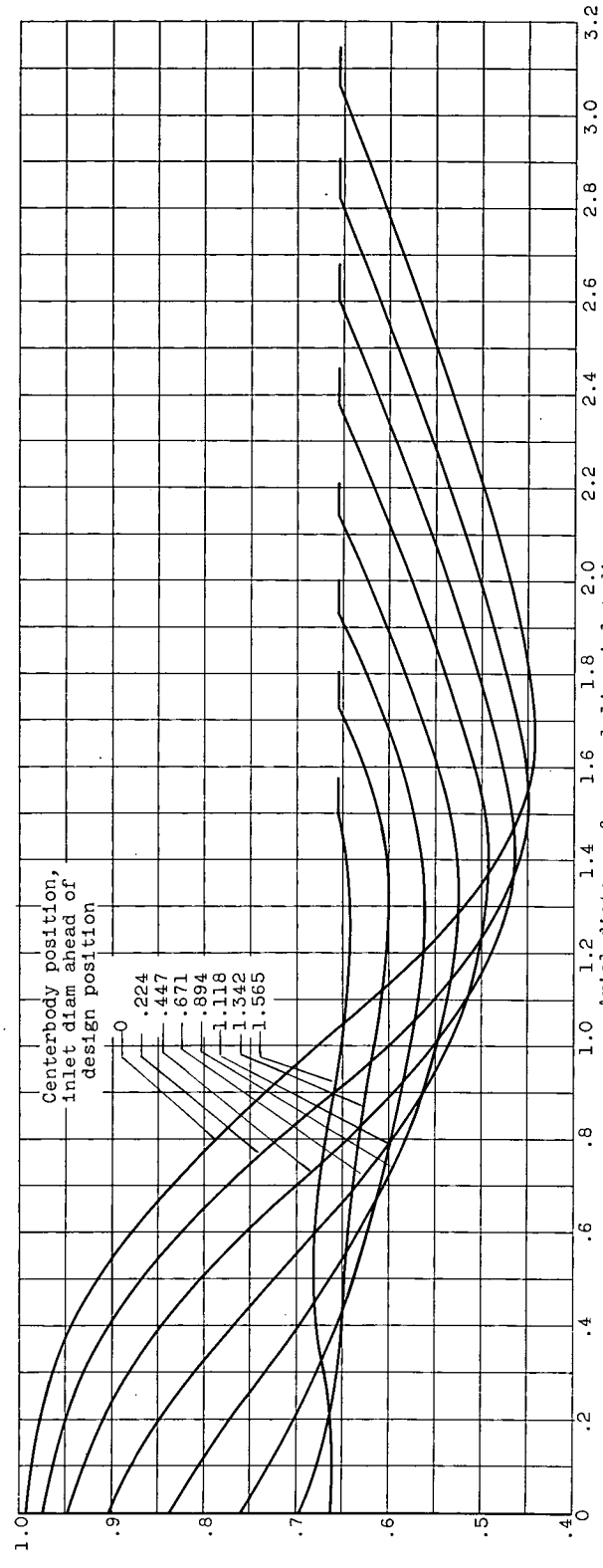


(a) For the original long inlet without constant-Mach-number section.

Figure 5. - Area distribution.

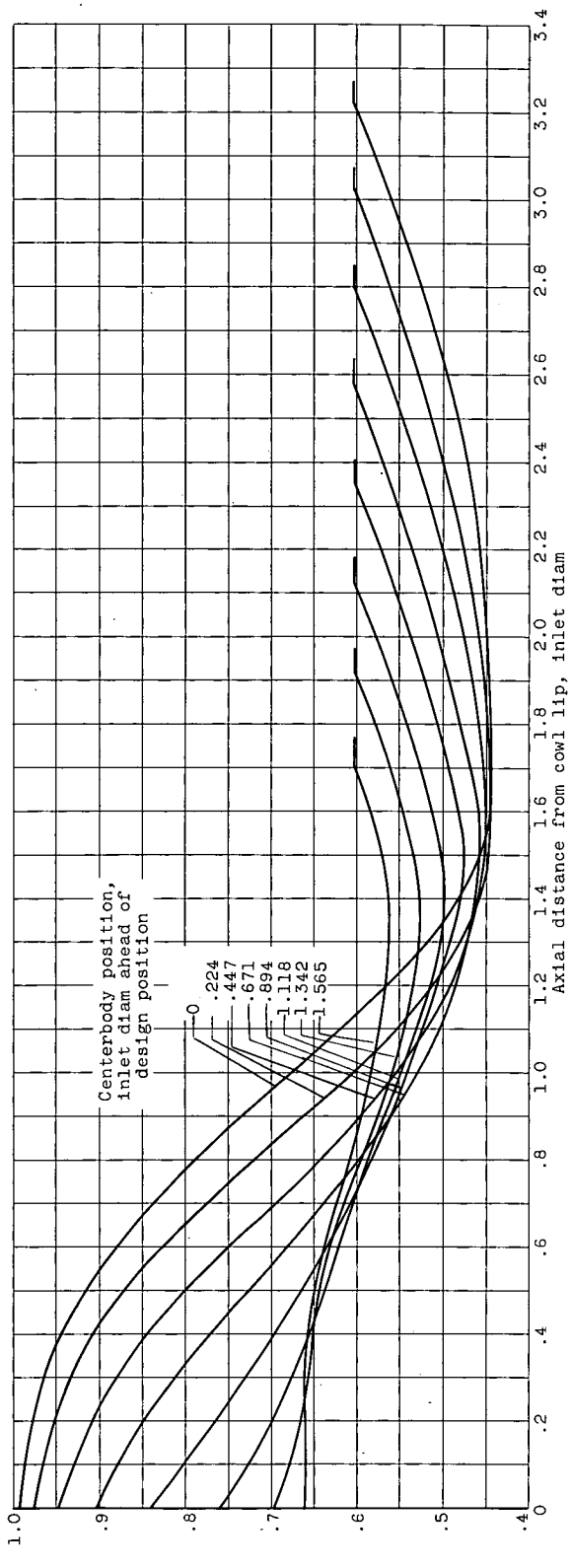


(b) For the original long inlet with constant-Mach-number section.

Figure 5. - Continued. Area distribution.

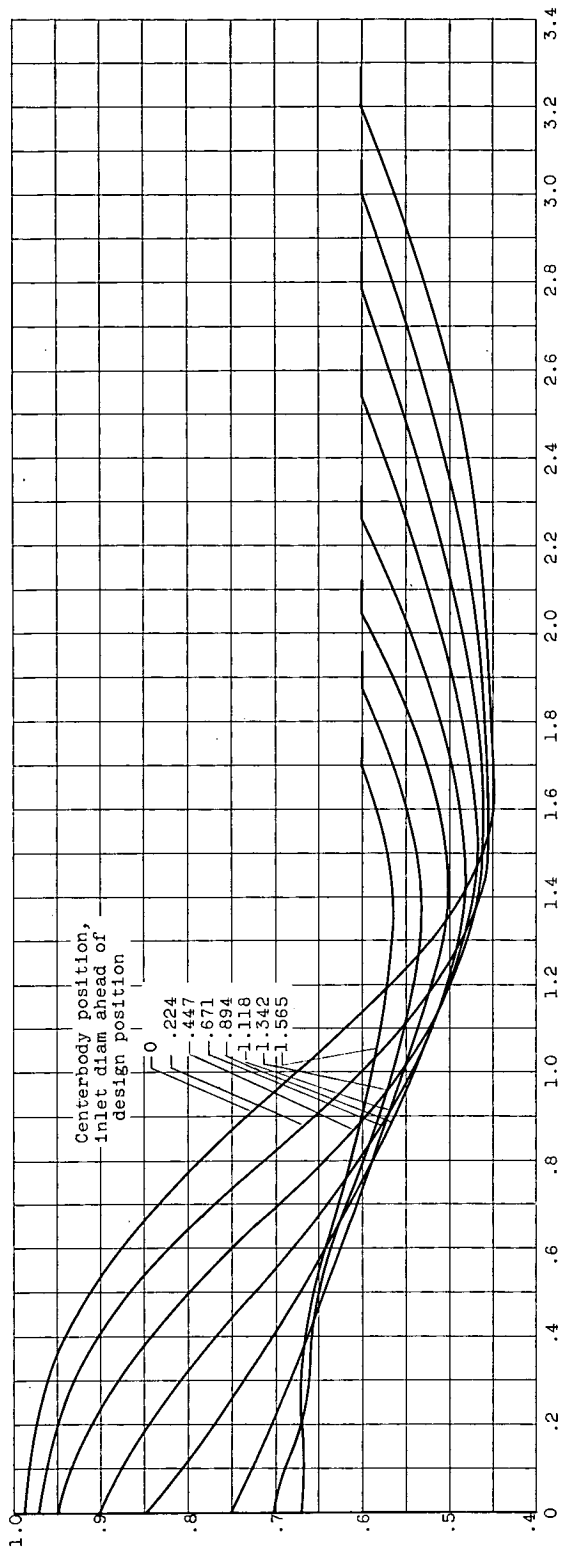


(c) For the modified long inlet with constant-Mach-number section.

Figure 5. - Concluded. Area distribution.

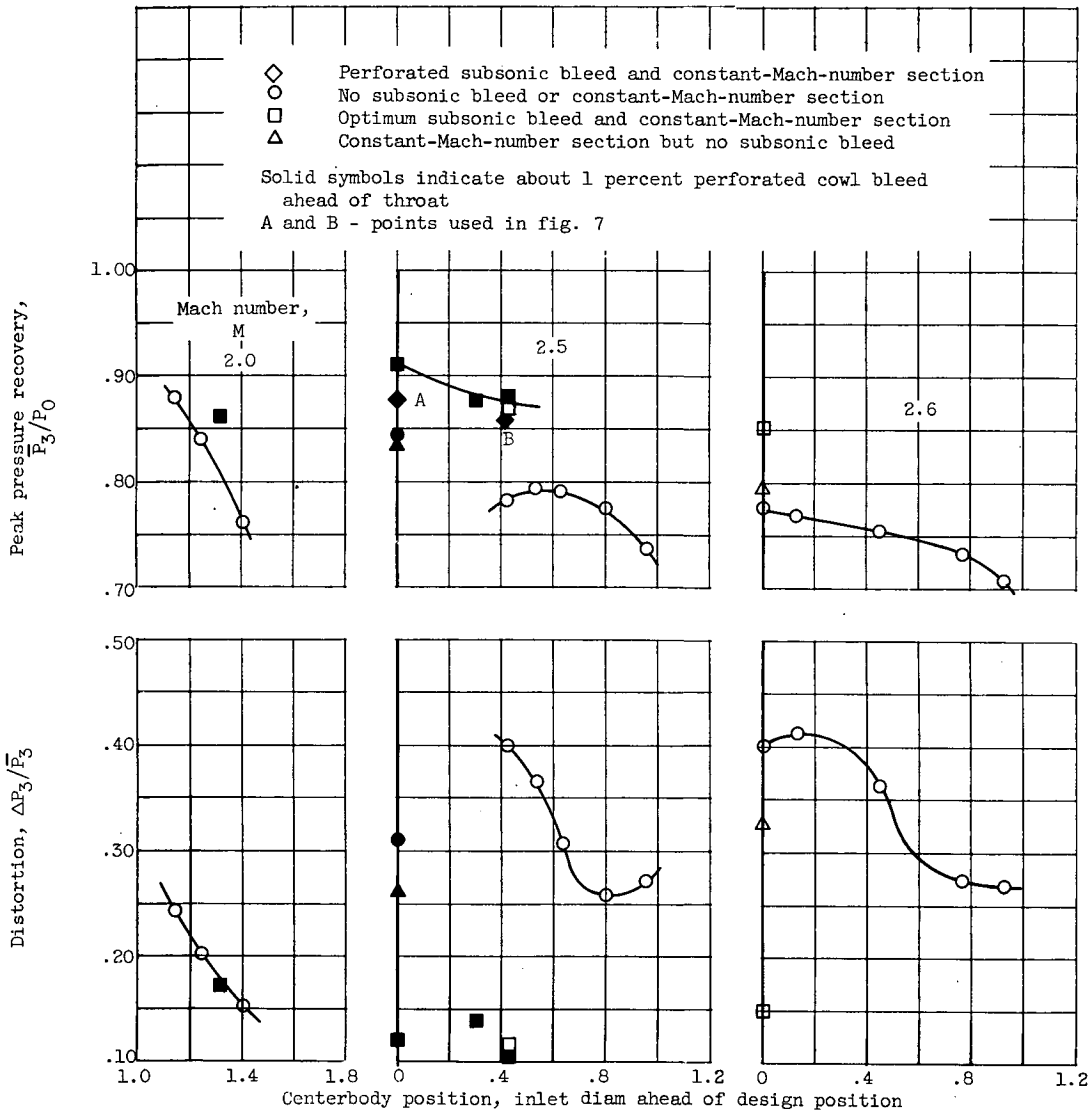


Figure 6. - Over-all inlet performance. Reynolds number, $2.5 \times 10^6$ per foot.

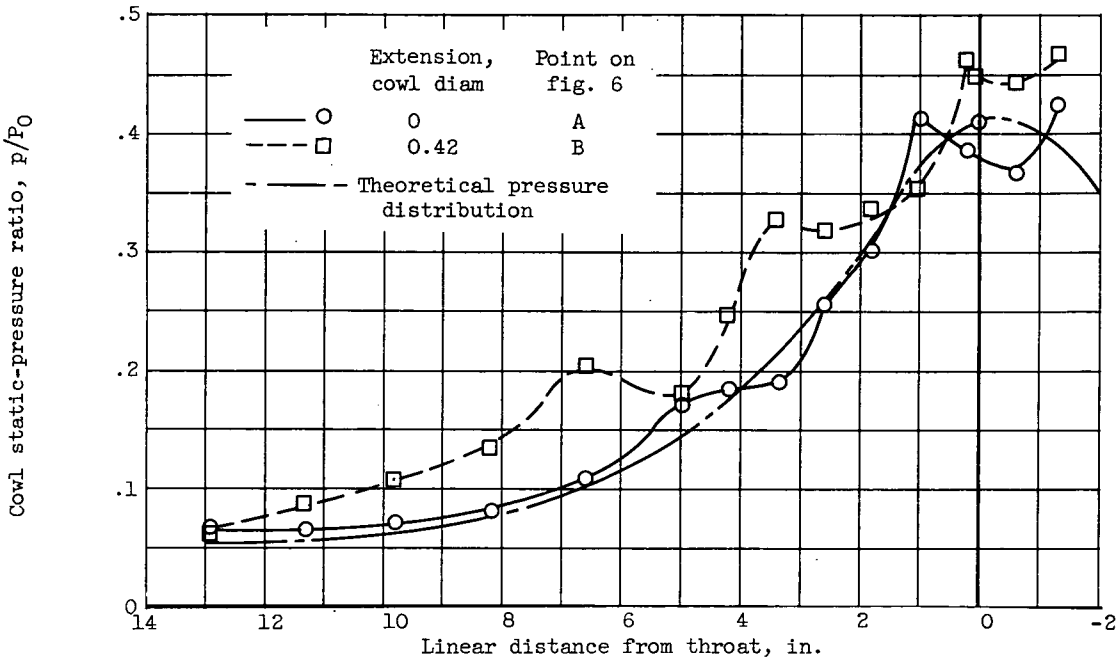


(a) Cowl static-pressure distribution.

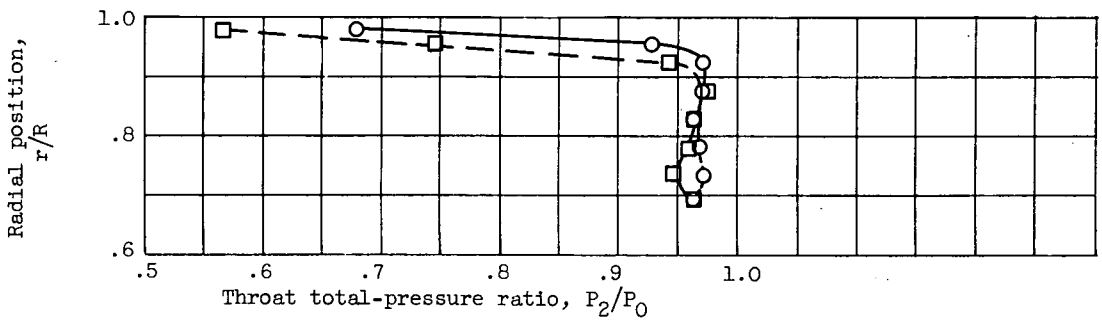


(b) Throat total-pressure profile.

Figure 7. - Effect of centerbody translation on supersonic performance of modified long inlet with subsonic perforated bleed. Mach number, 2.5; Reynolds number, $2.5 \times 10^6$ per foot.

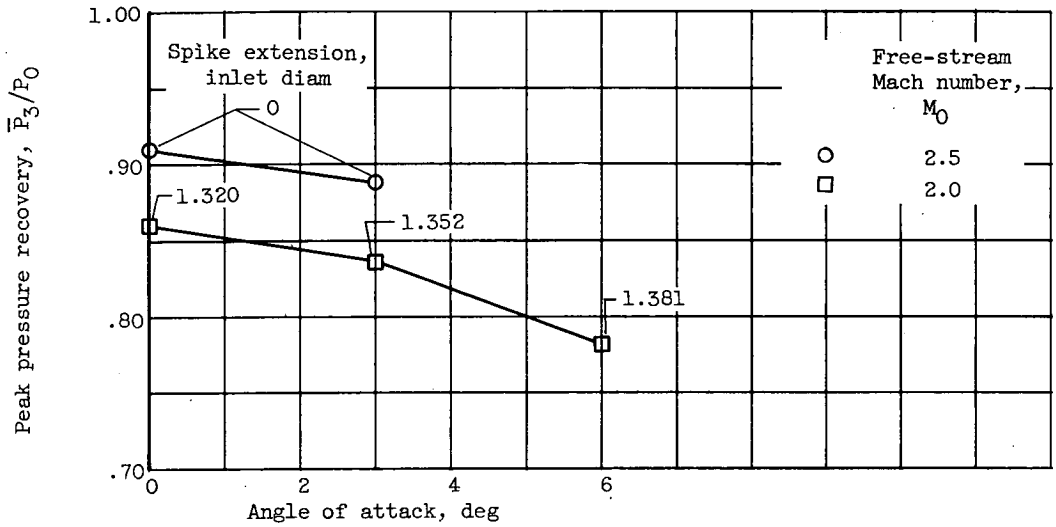


Figure 8. - Effect of angle of attack on peak pressure recovery (modified long inlet with forward enlarged cowl and original centerbody slots and constant-Mach-number section; Re, $2.5\times10^6$ per ft).

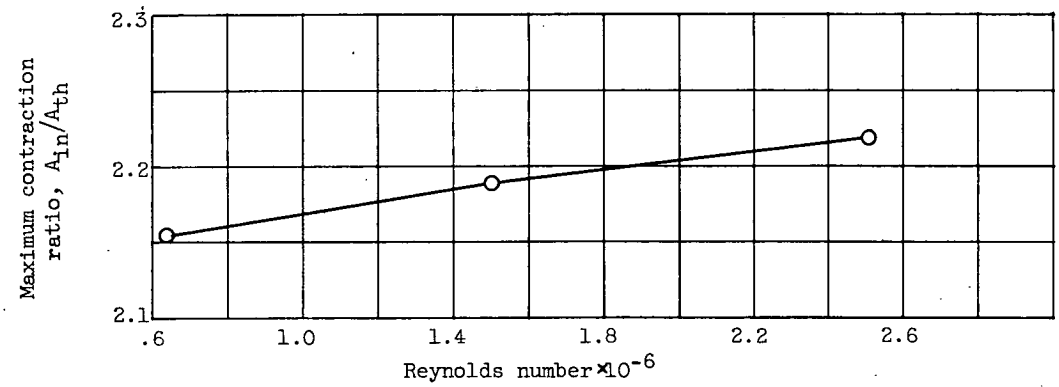


Figure 9. - Effect of Reynolds number on maximum obtainable contraction ratio at Mach 2.5 (modified long inlet with forward enlarged cowl and original centerbody slots and constant-Mach-number section).

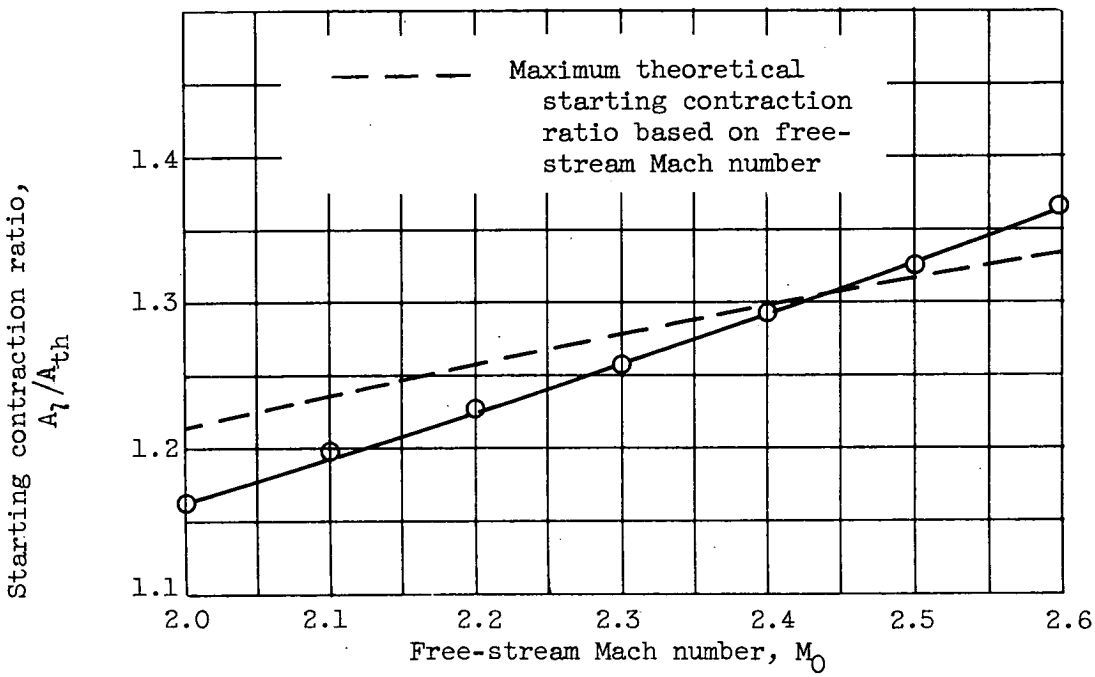


Figure 10. - Starting characteristics for the original long inlet with no constant-Mach-number section and no bleed. Reynolds number, $2.5 \times 10^6$ per foot.

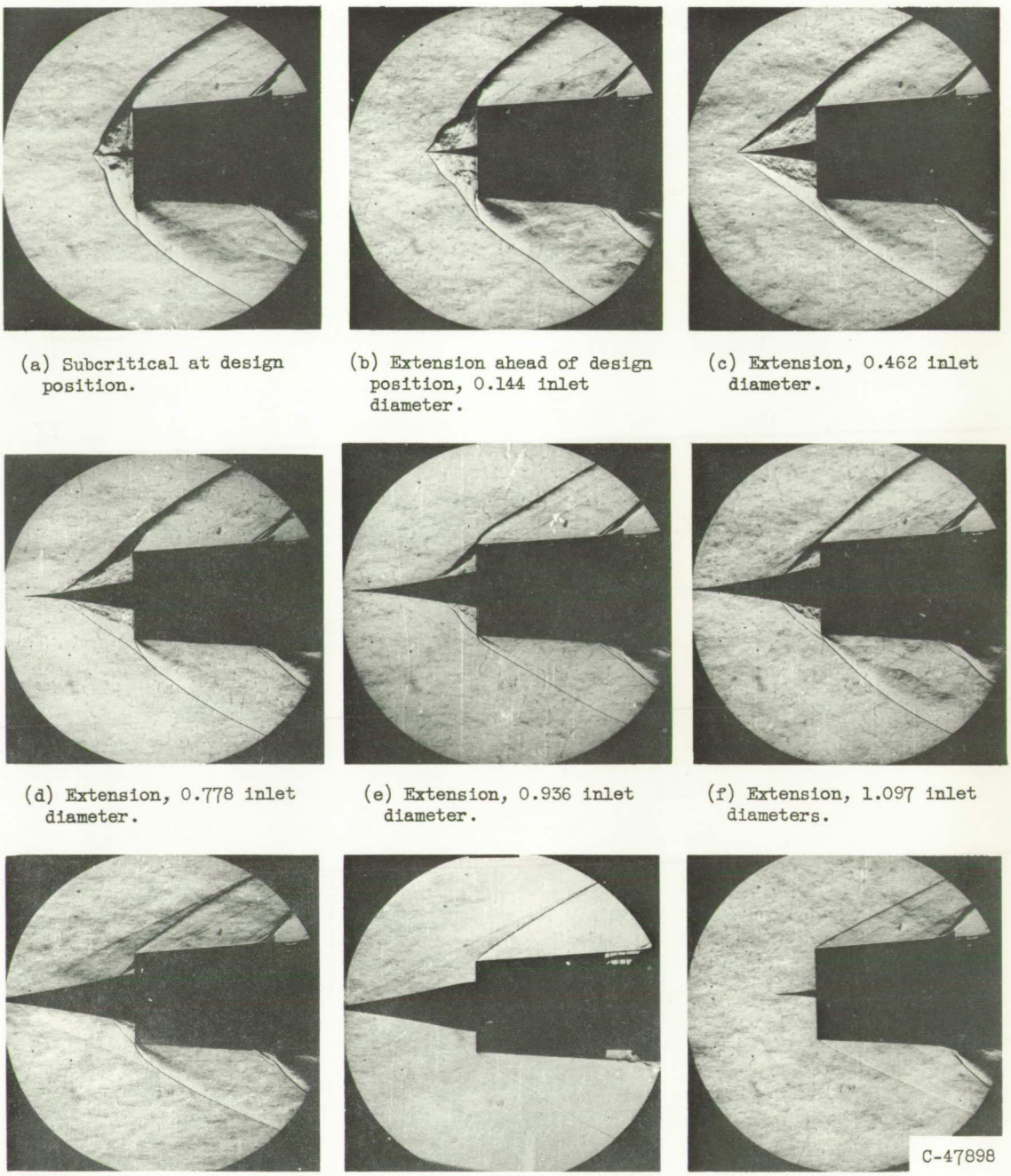


(a) Subcritical at design position.

(b) Extension ahead of design position, 0.144 inlet diameter.

(c) Extension, 0.462 inlet diameter.

(d) Extension, 0.778 inlet diameter.

(e) Extension, 0.936 inlet diameter.

(f) Extension, 1.097 inlet diameters.

(g) Extension, 1.320 inlet diameters.

(h) Minimum extension for starting, 1.337 inlet diameters.

(i) Supercritical at design position.

Figure 11. - Spark schlieren photographs of inlet starting at Mach 2.5. Reynolds number, $2.5 \times 10^6$ per foot.

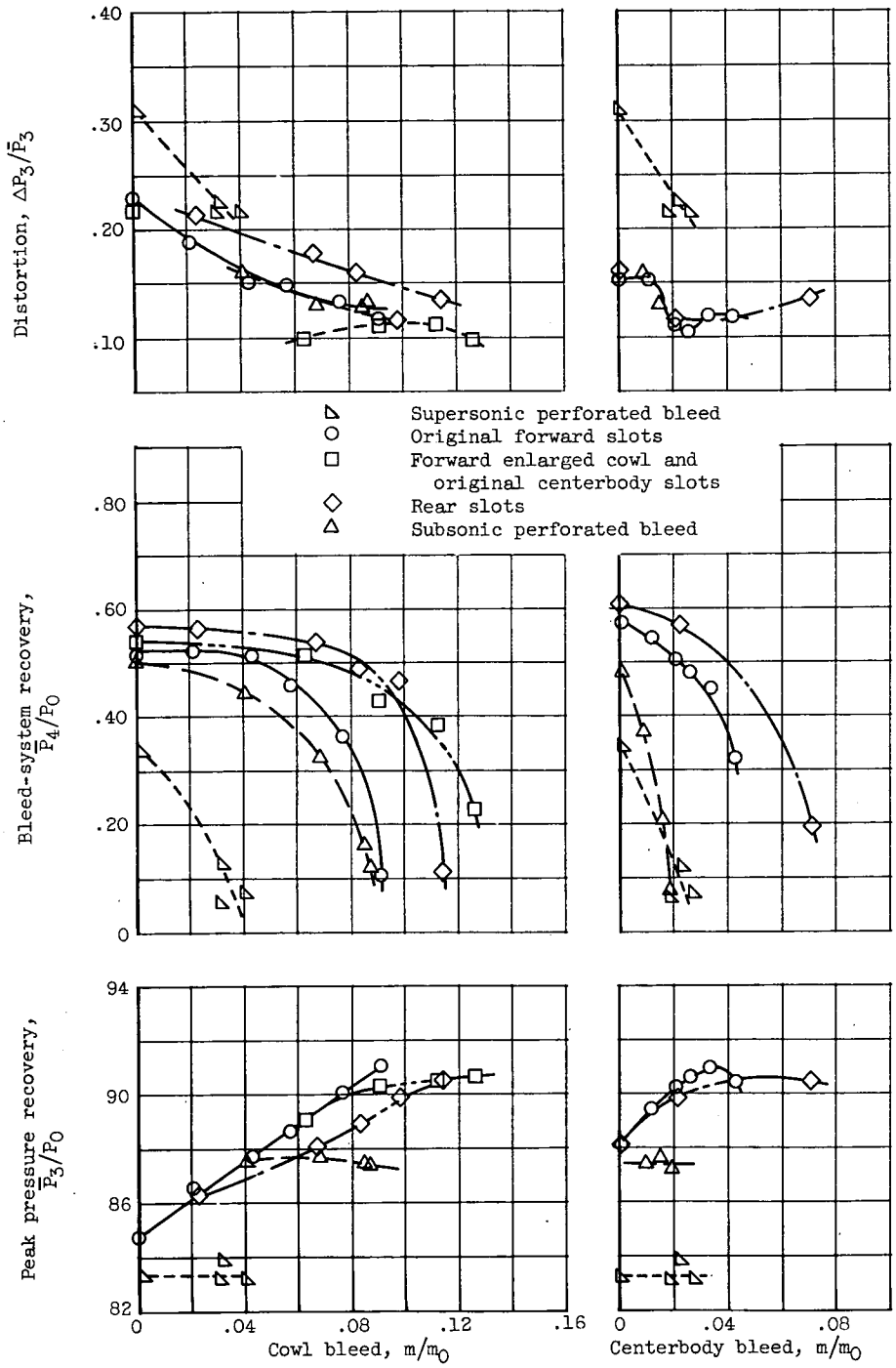


(a) Cowl-bleed performance for optimum centerbody-bleed flow.

(b) Centerbody-bleed performance for optimum cowl-bleed flow.

Figure 12. - Performance of bleed configurations. Mach number, 2.5; Reynolds number, $2.5 \times 10^6$ per foot.

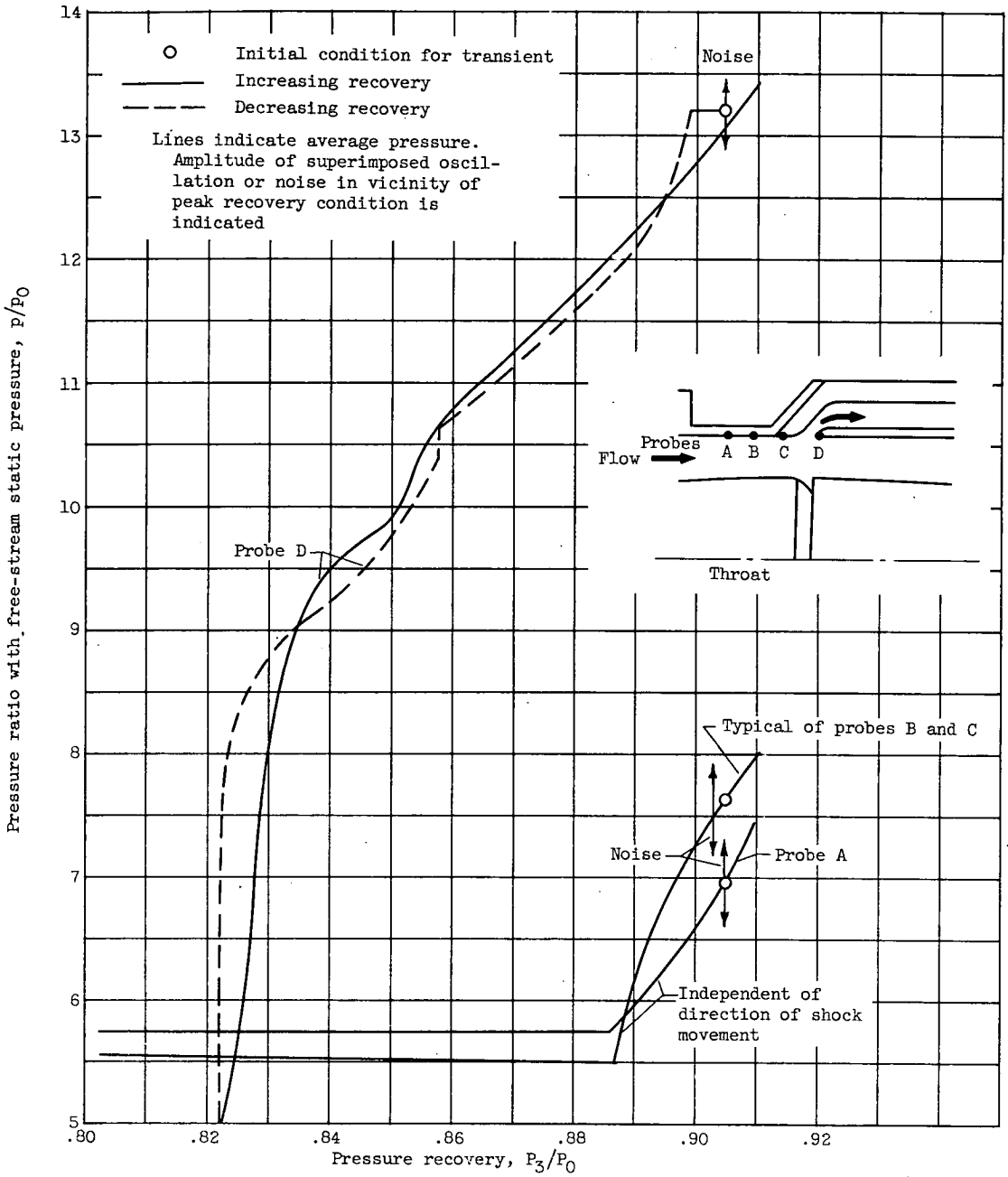


Figure 13. - Static pressure in region of forward slot (modified long inlet with forward enlarged cowl and original centerbody slots). Angle of attack, 0°; Mach number, 2.5; Reynolds number, $2.5 \times 10^6$ per foot.

NOTES: (1) Reynolds number is based on the diameter of a circle with the same area as that of the capture area of the inlet.

(2) The symbol * denotes the occurrence of buzz.

INLET BIBLIOGRAPHY SHEET

| Report and facility | Description: Configuration | Description: Number of oblique shocks | Description: Type of boundary-layer control | Test parameters: Free-stream Mach number | Test parameters: Reynolds number $\times 10^{-6}$ | Test parameters: Angle of attack, deg | Test parameters: Angle of yaw, deg | Test data: Drag | Test data: Inlet-flow profile | Test data: Discharge-flow profile | Test data: Flow picture | Performance: Maximum total-pressure recovery | Performance: Mass-flow ratio | Remarks |
|---|---|---|---|---|---|---|---|---|---|---|---|---|---|---|
| CONFID. RM E58E16 Lewis 10- by 10-ft supersonic wind tunnel | 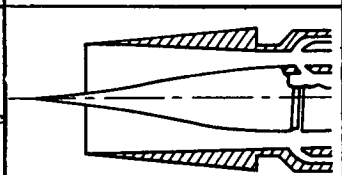 | Isen-tropic | (a) Flush slots downstream of throat. | 2.7<br>2.6<br>2.5 | 1.860<br>1.860<br>1.860 | 0<br>0<br>0 | 0<br>0<br>0 | | | | | <br>0.85<br>.91 | 1.0<br>1.0<br>1.0 | Axially symmetric inlet designed for isentropic contraction at Mach 2.5. |
| | | | | | 1.117 | 3 | 0 | | | | | | 1.0 | |
| | | | (b) Per-forated a-head and behind throat. | | 0.476 | - | 0 | | | | | | 1.0 | |
| | | | | 2.0 | 1.860 | 0, 3, 6 | 0 | | | | | .88 | 0.905 to 0.665 | |
| CONFID. RM E58E16 Lewis 10- by 10-ft super-sonic wind tunnel | 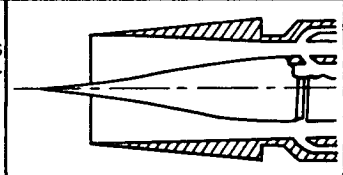 | Isen-tropic | (a) Flush slots downstream of throat. | 2.7<br>2.6<br>2.5 | 1.860<br>1.860<br>1.860 | 0<br>0<br>0 | 0<br>0<br>0 | | | | | <br>0.85<br>.91 | 1.0<br>1.0<br>1.0 | Axially symmetric inlet designed for isentropic contraction at Mach 2.5. |
| | | | | | 1.117 | 3 | 0 | | | | | | 1.0 | |
| | | | (b) Per-forated ahead and behind throat. | | 0.476 | - | 0 | | | | | | 1.0 | |
| | | | | 2.0 | 1.860 | 0, 3, 6 | 0 | | | | | .88 | 0.905 to 0.665 | |
| CONFID. RM E58E16 Lewis 10- by 10-ft super-sonic wind tunnel | 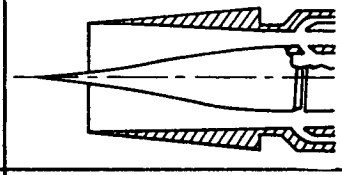 | Isen-tropic | (a) Flush slots downstream of throat. | 2.7<br>2.6<br>2.5 | 1.860<br>1.860<br>1.860 | 0<br>0<br>0 | 0<br>0<br>0 | | | | | <br>0.85<br>.91 | 1.0<br>1.0<br>1.0 | Axially symmetric inlet designed for isentropic contraction at Mach 2.5. |
| | | | | | 1.117 | 3 | 0 | | | | | | 1.0 | |
| | | | (b) Per-forated ahead and behind throat. | | 0.476 | - | 0 | | | | | | 1.0 | |
| | | | | 2.0 | 1.860 | 0, 3, 6 | 0 | | | | | .88 | 0.905 to 0.665 | |
| CONFID. RM E58E16 Lewis 10- by 10-ft super-sonic wind tunnel | 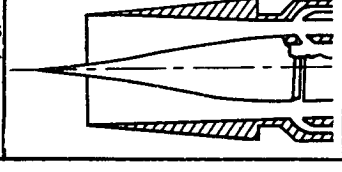 | Isen-tropic | (a) Flush slots downstream of throat | 2.7<br>2.6<br>2.5 | 1.860<br>1.860<br>1.860 | 0<br>0<br>0 | 0<br>0<br>0 | | | | | <br>0.85<br>.91 | 1.0<br>1.0<br>1.0 | Axially symmetric inlet designed for isentropic contraction at Mach 2.5. |
| | | | | | 1.117 | 3 | 0 | | | | | | 1.0 | |
| | | | (b) Per-forated ahead and behind throat. | | 0.476 | - | 0 | | | | | | 1.0 | |
| | | | | 2.0 | 1.860 | 0, 3, 6 | 0 | | | | | .88 | 0.905 to 0.665 | |

Bibliography

These strips are provided for the convenience of the reader and can be removed from this report to compile a bibliography of NACA inlet reports. This page is being added only to inlet reports and is on a trial basis.